WATER MASS FLOW OPTIMIZATION FOR HYDROSOLAR ROOF

Lucas M., Martínez P., Kaiser A. S., Viedma A., Zamora B.
Dpto. Ing. Térmica y de Fluidos. Universidad Politécnica de Cartagena

Campus Muralla del Mar C/ Dr Fleming, s/n

e-mail: manuel.lucas@upct.es

Abstract

Cooling towers are classical solutions to remove heat from air-conditioning systems and other industrial facilities. This process is possible due to the energy and mass transfer between flowing air and water. The hydrosolar roof optimised in this paper is able to obtain the same effect substituting the fan of the mechanical draught cooling towers for air flow induced by solar radiation and wind. In a previous work, the drop size of the sprayed water and the pumping pressure necessary to obtain it was studied and the optimal operation point was found to a fixed water mass flow. This work describes the design point optimization procedure taking into account the water mass flow as an essential variable to evaporative systems. In particular, air and water mass flow ratio is one of the most important variable to study the cooling capacity in a cooling tower. Therefore, hydrosolar roof results will be showed as cooling tower results are usually showed. The necessary correlations to performance the optimization procedure were obtained by a hydrosolar roof numerical modelization. The numerical simulation takes into account both evaporative and convective effects and two-dimensional version of the CFD code Fluent was used. In this way, weather variables as solar radiation, wind velocity, dry bulb temperature and wet bulb temperature have been taking into account. Numerical results have been validated with the experimental results obtained previously in a hydrosolar roof prototype.

(Keywords: Drop size, Air-conditioning, solar chimney, cooling tower, solar energy)

1. Introduction

A new system for buildings climatization has been studied during the last five years. It consists of an extended framework on the roof of the building with some thermal plates installed over it. Some of the plates are made of a high reflective material, and the others are made of absorbent material. The Hydrosolar Roof uses the design of the reflective and absorbent parts of the device, made of flat plates, to form a sloping channel. Solar radiation is collected by this channel and, due to local heating in this zone, natural convection through it is produced. The natural induced air flow is irrigated with water sprays, placed below the plates at the inlet of the channel, generating a cross flow between air and water. In this way, water is cooled by direct contact with a reduced amount of vaporization, and most of the water is recovered at a reduced temperature.

In the last years, it has been analysed by different authors. Kaiser and Viedma (2001) developed an experimental study of the first generation Hydrosolar Roof and showed its energy performance. Kaiser et al. (2001) (a) optimized the system heat dissipation and changed the Hydrosolar Roof design according to different parameters such as air mass flow and solar radiation, among others. Zamora et al. (2000) simulated the natural convection heat transfer in the solar chimney with Fluent, a CFD code, and they compared the numerical results with the experimental results. Kaiser et al. (2001) (b) numerically established the exhauster installation influence on the chimney outlet and the natural and forced air mass flow induced. Kaiser et al. (2002) simulated direct contact heat and mass transfer with the second generation Hydrosolar Roof using Fluent and they compared the numerical results with the experimental results obtained previously. Lucas et al. (2002) continued this work and studied the influence of the sprayed water drop size. They determined an optimum for this parameter in order to obtain a maximum in the power dissipated by the system. However, up to now, the influence of water mass flow and air mass flow ratio has not been considered. For this reason,

this paper shows the variation in the power dissipated as a function of this mass flow ratio. In order to study this influence, a total of forty five cases have been solved varying the water and air mass flow ratio m_w/m_a (0.5; 1; 1.5), the maximum gap of temperature ΔT_{max} (5; 10; 15) ºC and the water drop size ϕ (260; 463; 600; 730; 1000) μm. The CFD code Fluent was used for solving the cases above mentioned.

2. System Description

The Hydrosolar Roof is mounted on the roof of the buildings and is made of a metallic structure and an hydraulic circuit. The structure is composed of a framework made of steel, which gives support to both the set solar collector and the hydraulic subsystem. The interior space allows air to move across it from bottom to top without obstacles, but it can be considered divided into two different zones from a functional point of view. The upper part, known as convection zone, is made up of sloping channels whose walls are solar collector panels. The solar radiation impinges on these panels increasing their temperature above the environmental temperature. The air located inside the channels is heated by means of convection and the natural draft produces an upward air flow. Therefore, the upper zone basically is a solar chimney. The lower part, known as the evaporative cooling zone, has a series of nozzles that spray water crosscurrent the upward air flow. The water exchanges mass and energy with the air flow and is recovered colder. This zone works as a counter flow cooling tower. The whole system can be regarded as a two-dimensional solar chimney coupled to a widespread cooling tower.
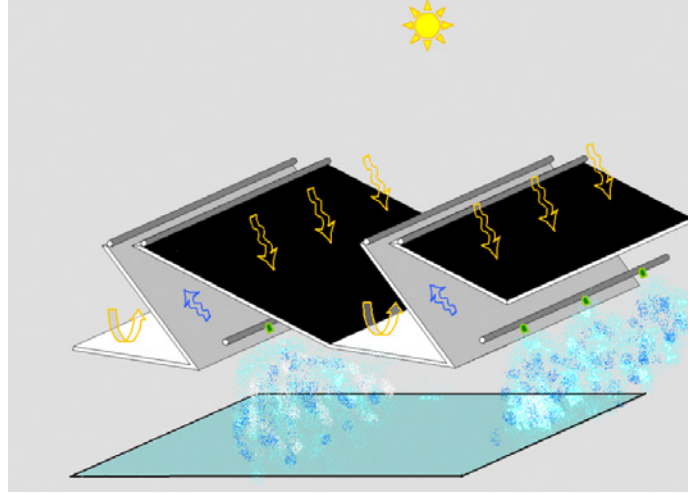

Figure 1: Hydrosolar Roof Sketch

3. Mathematical Model

In order to analyse the mathematical model of the problem that has been treated here, three groups of equations may be considered: the group of equations that govern the continuous phase (mass flow in the chimney produced by natural convection), the group of equations of the discrete phase (drops of water that has been sprayed), and the group of equations that provide the chemical species (dry air and water vapour). The continuous and discrete phase equations are coupled by the source terms of conservation equations. The equations of the continuous phase are represented below.

$$\frac{\partial \rho}{\partial t} + \frac{\partial}{\partial x_i}(\rho v_i) = S_{i'}, \tag{1}$$

$$\rho \frac{\mathrm{d} v_i}{\mathrm{d} t} = \frac{\partial}{\partial x_j}\left[\mu\left(\frac{\partial v_i}{\partial x_j} + \frac{\partial v_j}{\partial x_i}\right) - \frac{2}{3}\mu\left(\frac{\partial v_j}{\partial x_j}\right)\delta_{ij}\right] + \rho f_{mi} - \frac{\partial P}{\partial x_i} + F_i, \tag{2}$$

$$\rho\left(\frac{\partial e}{\partial t} + v_i \frac{\partial e}{\partial x_i}\right) = -p \frac{\partial v_i}{\partial x_i} + \Phi_v + \frac{\partial}{\partial x_i}\left(k \frac{\partial T}{\partial x_i}\right) + \frac{\partial}{\partial x_i}\left(\sum_{j=1}^{n} h_{j'} J_{j'}\right) + S_h, \tag{3}$$

$$\rho\left(\frac{\partial m_{i'}}{\partial t} + v_i \frac{\partial m_{i'}}{\partial x_i}\right) = -\frac{\partial J_{i',i}}{\partial x_i} + S_{i'}, \tag{4}$$

$$J_{i',i} = -\rho D_{i',m} \frac{\partial m_{i'}}{\partial x_i}, \tag{5}$$

where $S_{i'}$, F_i y S_h represent the source terms, $m_{i'}$ is the local mass fraction of the specie i', $\sum_{j=1}^{n} h_{j'} J_{j'}$ is enthalpy transport due to diffusion of specie j', $J_{i',i}$ is the diffusion flux of specie i', and $D_{i',m}$ is the diffusion coefficient of specie i' in the mixture.

The trajectory of a discrete phase particle (droplet) may be predicted by integrating the force balance on the particle, which is written in a Lagrangian reference frame. This force balance equates the particle inertia with the forces acting on the particle, and can be written (for the x direction in Cartesian coordinates) as equation (6). On the other hand, energy balance for the particle is also considered in equation (8).

$$\frac{\mathrm{d} u_{pi}}{\mathrm{d} t} = \frac{18\mu}{\rho_p D_p^2} \frac{C_D \operatorname{Re}}{\partial x_i}\left(v_i - u_{pi}\right) + g_i \frac{(\rho_p - \rho)}{\rho_p} + \frac{\rho}{\rho_p} u_{pi} \frac{\partial v_i}{\partial x_i}, \tag{6}$$

$$\frac{\mathrm{d} x_i}{\mathrm{d} t} = u_p \tag{7} \qquad m_p C_p \frac{\mathrm{d} T_p}{\mathrm{d} t} = h A_p (T_\infty - T_p) + \frac{\mathrm{d} m_p}{\mathrm{d} t} h_{fg}, \tag{8} \qquad \operatorname{Re} = \frac{\rho D_p (u_{pi} - v_i)}{\mu}, \tag{9}$$

$$C_D = a_1 + \frac{a_2}{\operatorname{Re}} + \frac{a_3}{\operatorname{Re}^2}, \tag{10} \qquad F_D = \frac{18\mu}{\rho_p D_p^2} \frac{C_D \operatorname{Re}}{\partial x_i}, \tag{11}$$

where a_i´s coefficients are constants that apply for smooth spherical particles over several ranges of Re given by Morsi and Alexander (1972), $F_D(v_i\text{-}u_{pi})$ is the drag force per unit particle mass, $g_i(\rho_p\text{-}\rho)/\rho_p$ is the gravity force per unit particle mass, and $(\rho/\rho_p)u_{pi}(\partial v_i/\partial x_i)$ is the force due to the pressure gradient in the fluid, where v_i and ρ are the velocity and density in the continuous phase; u_{pi}, ρ_p, m_p, T_p, h_{fg} y C_p the velocity, density, mass, temperature, latent heat, heat capacity of the particle, h the convection heat transfer coefficient and $\mathrm{d}m_p/\mathrm{d}t$ the rate of evaporation in the particle.

The process of coupling between discrete and continuous phase are solved by an iterative method. As the trajectory of a particle is computed, the code keeps track of the heat, mass, and momentum gained or lost by the particle stream that follows that trajectory and these quantities can be incorporated in the subsequent continuous phase calculations. Thus, while the continuous phase always impacts the discrete phase, you can also incorporate the effect of the discrete phase trajectories on the continuum. This two-way coupling is accomplished by alternately solving the discrete and continuous phase equations until the solutions in both phases have stopped changing. The source term in the continuity conservation equation my be written as

$$S_{i'} = \frac{\Delta m_p \dot{m}_{p_o}}{m_{p_o}\, d\forall}, \tag{12}$$

where Δm_p is change in the mass of the particle in the control volume in a dt, $\dot{m}_{p_o}$ initial mass flow rate of the particle injection tracked and m_{p_o} the initial mass of the particle. The mass evaporated may be expressed by

$$\Delta m_p (d\forall) = m_p(t) - m_p(t - dt) = N_{i'} M_{i'} A_p\, dt, \tag{13}$$

where $dt = ds/(u_p + v)$, and ds is the fraction of trajectory incide of each $d\forall$ considered; $M_{i'}$ is the molecular weight of specie i', A_p the droplet area and $N_{i'}$ the molar flux of vapour:

$$N_{i'} = K_c \left(C_{i',s} - C_{i',\infty} \right), \tag{14}$$

where $C_{i',s}$ is the vapor concentration at the droplet surface and $C_{i',\infty}$ vapour concentration in the bulk gas:

$$C_{i',s} = \frac{P_{sat}(T_p)}{R(T_p)} \qquad C_{i',\infty} = \frac{P_\infty x_{i'}}{RT_\infty}. \tag{15}$$

where $x_{i'}$ is the mass fraction of the specie i'. The mass transfer coefficient K_c is obtained by a correlation of Nusselt number given by Ranz y Marshall (1952) (a) y (b)

$$K_c = \frac{Nu\, D_{i',m}}{D_p} = \frac{\left(2 + 0{,}6 \cdot Re^{1/2} S_c^{1/3}\right) D_{i',m}}{D_p}, \tag{16}$$

The source terms of momentum equation, F_i, and energy equation are given by the expressions

$$F_i = \left(\frac{18\mu}{\rho_p D_p^2} \frac{C_D Re}{\partial x_i} (v_i - u_{p_i}) + g_i \frac{(\rho_p - \rho)}{\rho_p} + \frac{\rho}{\rho_p} u_{p_i} \frac{\partial v_i}{\partial x_i} \right) \frac{\dot{m}_{p_o}\, dt}{d\forall} \tag{17}$$

$$S_h = \left[\frac{\overline{m}_p}{m_{p_o}} C_p \Delta T_p + \frac{\Delta m_p}{m_{p_o}} \left(-h_{fg} + h_{pyrol} + \int_{T_{ref}}^{T_p} C_{p,i}\, dT \right) \right] \frac{\dot{m}_{p_o}}{d\forall}, \tag{18}$$

where D_p is the diameter of the droplet and $\dot{m}_{p_o}$ is the mass flow of particles contained in that differential of volume, $\overline{m}_p$ the average mass of the particle in the control volume $d\forall$, m_{p_o} the initial mass of the particle, C_p the heat capacity of the particle, ΔT_p the temperature change of the particle in the control volume in the $d\forall$, Δm_p the change in the mass of the particle in the control volume $d\forall$, h_{fg} the latent heat of volatiles evolved, h_{pyrol} the heat of pyrolysis as volatiles are evolved, $C_{p,i}$ the heat capacity of the volatiles evolved, T_p the temperature of the particle upon exit of the control volume $d\forall$ and T_{ref} the reference temperature for enthalpy.

This equations system has been solved numerically by a 2D model with a finite volumes code (Fluent). A sensibility study of the grid size was carried out, and the optimal

one was formed by 24.208 cells. The discretization scheme of the numerical model was "Presto" and a first order upwind scheme was used for the convective terms. The coupling between momentum and continuity equation by means of pressure was solved by the "Simple" algorithm of Patankar (1980).

4. Numerical Results

The aim of this section is to show all the numerical results obtained as a starting point of the optimization procedure. Previous study was only interested in the influence on efficiency of one thermodynamic parameter (maximum water temperature difference by means of varying inlet water temperature and fixing ambient wet bulb temperature) and one geometric parameter (drop size). Efficiency is an usual parameter to define the cooling tower capacity. In this work, 45 cases have been calculated to simulate the effect of modifying water mass flow (3 different water mass flow, 5 water drop size and 3 maximum water temperature difference values). To different water mass flow, different water and air mass flow ratio was obtained. This value only was calculated after numerical solution because air mass flow was a result of the calculations. In Mohiuddin and Kant (1996) is described the characteristic working zone ratio belonging to [0.5, 3], therefore this is the studied interval. Next figures show an example of the results obtained with the numerical calculations.
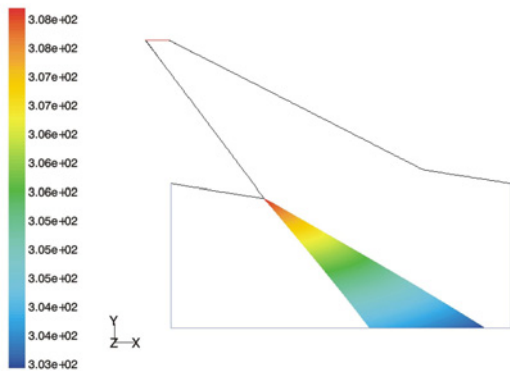

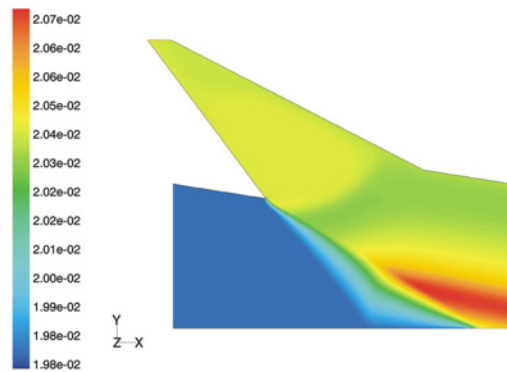Figure 2: Water temperature evolution (K)

Figure 3: Water mass fraction

With the finite volumes code water outlet temperature is calculated t a defined case. Once, this value is known, efficiency can be calculated. All the efficiency results and the correlations obtained are showed in the next figures
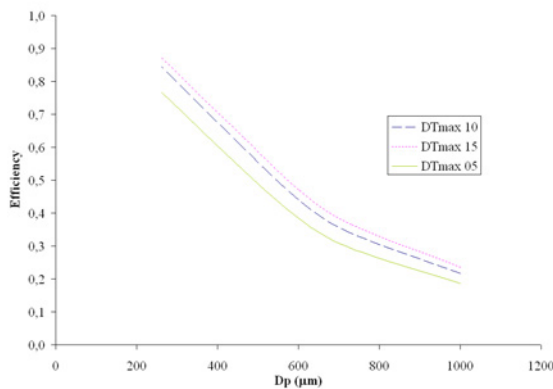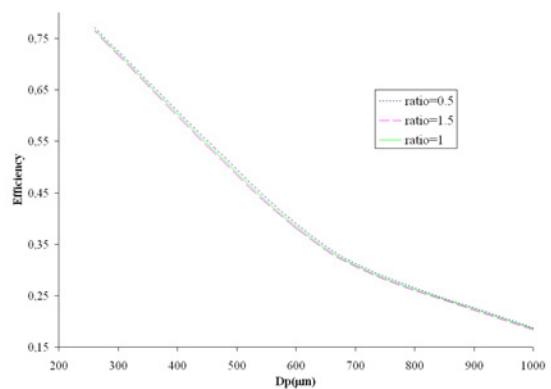

Figure 1: Efficiency vs. Drop size & ΔTmax

Figure 2: Efficiency vs. Drop size & ratio $\left(\dot{m}_w/\dot{m}_a\right)$

From the results, it can be observe the slight inverse relation between ratio and efficiency. Numerical results are in accordance with experimental results since the grater the ratio is, the lower the efficiency is. All the calculated data has been correlated to obtain and useful efficiency function to the optimization procedure.

5. Optimization and discussion

Following optimization procedure is valid for any hydrosolar roof, however, all the data presented in this paper is calculated, as a example, to the prototype installed at Technical University of Cartagena (Spain) with a total occupied surface of 36 m^2.

To characterize the piping installation a commercial software was used. This tool was useful to obtain the relation between water mass flow and pumping pressure, taking into account geometrical data, materials, and accessories. In M. Sánchez et al. (2002) there is a detailed explanation of the prototype technical information.
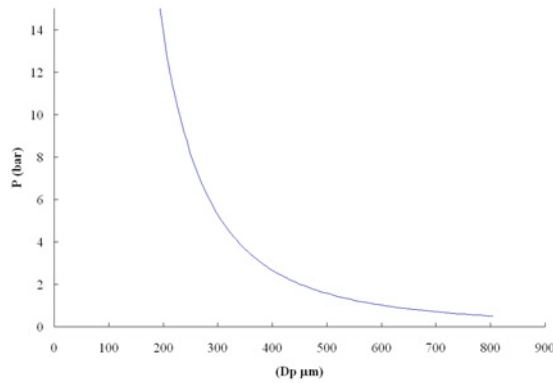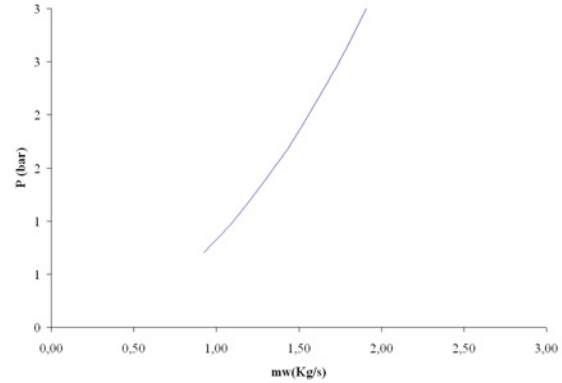

Figure 3: Water Drop Size vs. Pumping Pressure   Figure 4: Water Mass Flow vs. Pumping Pressure

In the previous work a dependence between water drop size and pumping pressure was obtained using nozzle manufactures information. At this moment, it is possible to obtain, for a pressure value, both water drop size sprayed and water mass flow per surface unit. Table 1 shows all the data calculated. Starting value is the cooling power of the cooling machine, and the modelization of the chiller is the same used in the previous work. With a chiller standard values using R-134a of useful overheating (4ºC) and useless overheating (3ºC) at the evaporator exit, pressure drops through suction line (9800 Pa) and discharge line (19600 Pa), underheating at condenser exit (2ºC) mechanical-electrical compressor efficiency (0.92) and isentropic compressor efficiency (0.9) and with a constant evaporator temperature (4.5 ºC), coefficient of performance is correlated with condensation temperature.

P(bar)	0,7	1,0	1,6	1,8	2,0	2,7	5,3
Diam	700,0	600,0	500,0	475,0	450,0	400,0	300,0
mw(Kg/s)	0,9	1,1	1,4	1,5	1,6	1,8	2,5
W pumping	65,7	114,0	218,7	262,7	318,7	485,6	1357,7
Efficiency	0,4	0,4	0,5	0,5	0,5	0,6	0,7
Twb	25,6	25,6	25,6	25,6	25,6	25,6	25,6
Tin	38,9	35,0	32,1	31,4	30,9	29,9	28,2
Dtmax	13,3	9,4	6,5	5,8	5,3	4,3	2,6
DT	5,1	4,1	3,3	3,1	2,9	2,5	1,8
Tout	33,9	30,9	28,8	28,4	28,0	27,4	26,5
Tcond	38,9	35,9	33,8	33,4	33,0	32,4	31,5
Tevap	4,5	4,5	4,5	4,5	4,5	4,5	4,5
COP (Real)	4,5	5,1	5,6	5,8	5,9	6,0	6,3
Qcond(w)	19569,6	19138,6	18854,1	18801,0	18753,9	18675,2	18564,4
W Comp.	3551,5	3120,4	2835,9	2782,8	2735,7	2657,0	2546,3
Qevap(w)	16018,2	16018,2	16018,2	16018,2	16018,2	16018,2	16018,2
W Total	3617,2	3234,4	3054,6	3045,6	3054,5	3142,5	3904,0
Cop (Global)	4,43	4,95	5,24	5,26	5,24	5,10	4,10

Table 1. Optimization data

By means of the inlet water conditions, that is, mass flow, temperature and drop size; and ambient conditions, efficiency is obtained. At this point, it is important to emphasize the fact that in this work a variable water mass flow was calculated in front of the previous work where a constant inlet water pressure per unit of surface was calculated. Water outlet temperature is deduced from the efficiency and, then, condensation temperature with a standard difference between refrigerant and water. With evaporation and condensation temperature it is possible to calculate the coefficient of performance (COP Cycle) and the energy exchange in the refrigeration cycle. After that, a global coefficient of performance (COP Global) is defined as the relation of absorbed energy from the cold region and the consumed energy by the compressor and the pump. In case of being interested in another installation, to change the parameter referred to the water mass flow-pumping pressure curve will be enough.

The optimization process includes opposite effects. On the one hand, the higher the pumping pressure is, the lower the water drop size diameter is and the better the efficiency; on the other hand, the higher the pumping pressure is, the higher the pumped water mass flow is and the lower the efficiency. In this way, it is not clear the dependence between water pumping pressure and efficiency. Taking into account the interval studied, it can be concluded that to increase the pumping pressure leads to higher efficiency. However, it is important to say that this performance is limited by air saturation, and it is showed in Figure 5, where the increment of efficiency is less significant as water mass flow goes on. As well as Figure 5, Figure 6 shows the asymptotic performance of the condensation temperature to greater pumping pressure.
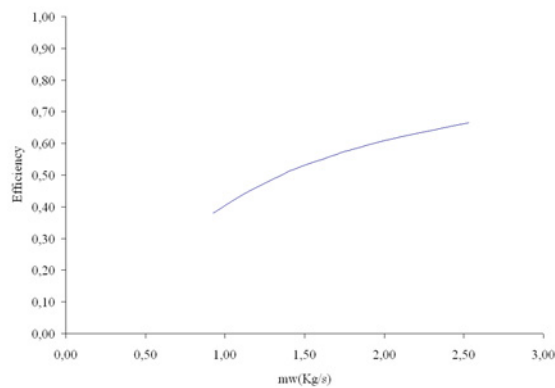
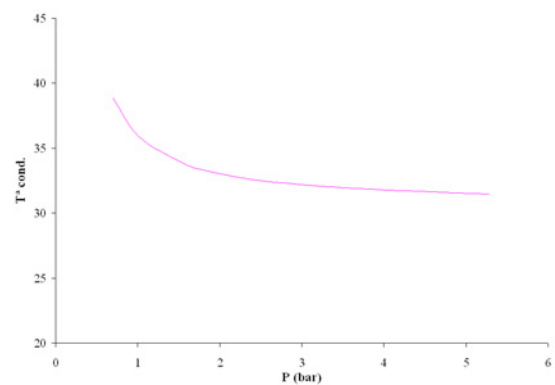**Figure 5: Efficiency vs. Water mass flow**

Figure 6: Condensation Temperature vs. Pumping Pressure

Optimization real sense is obtained when all the energy consumptions are considered. On the one hand, energy consumption related to the cooling machine, and on the other, energy consumption related to the hydrosolar roof. As the pressure is higher, obviously, the pumping energy is higher too, but the power consumed by the chiller compressor is lower because of the higher efficiency of the solar roof and the lower condensation temperature.
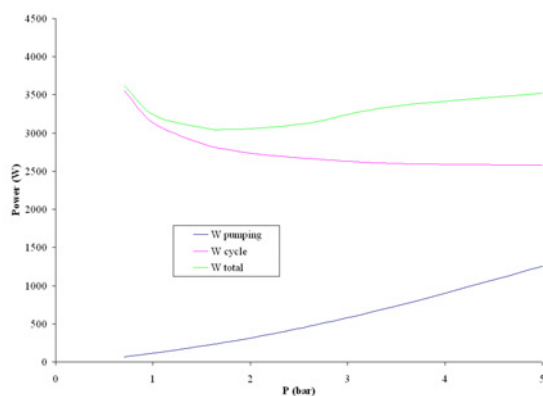

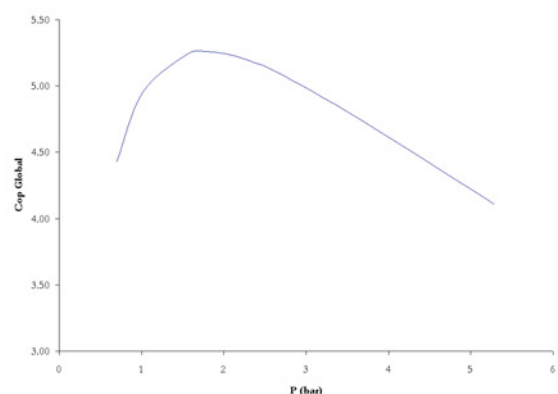**Figure 7: Energy Consumptions vs. Pumping pressure**

Figure 8: COP Global vs. Pumping pressure

In view of the fact that global coefficient of performance (COP Global) is defined as the relation of absorbed energy from the cold region and the consumed energy by the compressor and the pump, this parameter reflects the different tendencies of the energy consumptions. Since cooling capacity has been considered constant in this studied, maximum Global COP coincides with the point of lower energy consumption. In this case, the recommended water pumping pressure is 1,8 bar.

6. Conclusions

Conclusions achieved in this study can be summarized as follows:
- Hydrosolar second generation Roof direct contact heat and mass transfer simulation have been developed with a CFD code. In this new work, special attention has been

paid to water mass flow influence on the efficiency.

- Water mass flow optimization has been carried out and it has been necessary to include nozzle catalogue information, hydraulic installation description and a vapour compression refrigeration cycle model.
- Optimum coefficient of performance with a pumping pressure of 1.8 bar has been found to the prototype characteristic. A generalization procedure have been showed.
- As future studies can be planned a 3D simulation to take into account sprayed water, induced air distributions and direction of the wind.

7. Acknowledgements

8. References

Kaiser, A. S., Viedma, A., 2001, Hydrosolar roof for integrated energy dissipation and capture in buildings, Energy and Building, No.33, pp. 673-682.

Kaiser, A. S., Martínez, P., Lucas, M., Viedma, A., (a) 2001, Presentación del Prototipo de Techo Hídrico solar para la evacuación y captura de energía térmica en climatización de edificios, I Encuentro RIRAAS, Sevilla.

Zamora, B., Kaiser, A. S., Martínez, P., Lucas, M., 2000, Simulación numérica de la convección natural en una chimenea hídrico-solar, Fluent Users Meeting, Barcelona.

Kaiser, A S., Lucas, M., Zamora, B., (b) 2001, Estudio de extractores estáticos para la optimización del gasto en una chimenea hídrico-solar, Fluent Users Meeting, Madrid.

Kaiser, A S., Lucas, M., Martínez, P.,Viedma, A., Zamora, B., 2002, Simulación numérica de la transmisión de calor por evaporación producida en una torre de refrigeración extendida, CYTEF, Cartagena, Abril.

Lucas M., Martínez P., Kaiser A. S., Viedma A., Zamora B., 2002, water drop size numerical optimization for hydrosolar roof, Eurosun2002, Bologna.

Morsi, S. A., Alexander, A. J., 1972, An Investigation of Particle Trajectories in Two-Phase Flow Systems. J. Fluid Mech., 55(2):193--208, September 26.

Ranz, W. E., Marshall, W. R., (a) 1952, Evaporation from Drops, Part I. Chem. Eng. Prog., 48(3):141--146, March.

Ranz, W. E., Marshall, W. R., (b) 1952, Evaporation from Drops, Part II. Chem. Eng. Prog., 48(4):173--180, April.

Patankar, S. V., (1980).Numerical Heat Transfer and Fluid Flow. Hemisphere, Washington.

Ashrae Handbook., 1996, HVAC System and Equipment, Chap. 36.

Mohiuddin, A. K. M., Kant, K., 1996, Knowledge base for the systematic design of wet cooling towers, I. J. Refrig, V. 19, No. 1, pp. 43-51.

M. Sánchez et al., 2002, Climatic Solar Roof: An Ecological Alternative To Heat Dissipation In Buildings, Solar Energy Vol. 73, No. 6, pp. 419–432.